Advances in Applied Mathematics and Mechanics
Adv. Appl. Math. Mech., Vol. **9**, No. 6, pp. 1438-1460

DOI: 10.4208/aamm.OA-2016-0115
December 2017

Analysis of Mathematics and Numerical Pattern Formation in Superdiffusive Fractional Multicomponent System

Kolade M. Owolabi and Abdon Atangana*

Institute for Groundwater Studies, Faculty of Natural and Agricultural Sciences, University of the Free State, Bloemfontein 9300, South Africa

Received 9 September 2016; Accepted (in revised version) 20 January 2017

Abstract. In this work, we examine the mathematical analysis and numerical simulation of pattern formation in a subdiffusive multicomponents fractional-reaction-diffusion system that models the spatial interrelationship between two preys and predator species. The major result is centered on the analysis of the system for linear stability. Analysis of the main model reflects that the dynamical system is locally and globally asymptotically stable. We propose some useful theorems based on the existence and permanence of the species to validate our theoretical findings. Reliable and efficient methods in space and time are formulated to handle any space fractional reaction-diffusion system. We numerically present the complexity of the dynamics that are theoretically discussed. The simulation results in one, two and three dimensions show some amazing scenarios.

AMS subject classifications: 35A05, 35K57, 65L05, 65M06, 93C10

Key words: Asymptotically stable, coexistence, Fourier spectral method, numerical simulations, predator-prey, fractional multi-species system.

1 Introduction

Multicomponents system where species share common resources have drawn much attention of researchers dated to the pioneering work of Holt [33] based on apparent competition [41, 45, 56, 61]. Over the years, reaction-diffusion systems arise from the study of multi-species Lotka-Volterra interactions such as the predator-prey, competition, mutuality and food-chain models have been the subject of great interests [15, 18, 21, 25, 33, 37, 38, 41, 51]. Recently, many authors studied three-species population dynamics with various

*Corresponding author.
Emails: mkowolax@yahoo.com (K. M. Owolabi), abdonatangana@yahoo.fr (A. Atangana)

 ©2017 Global Science Press

https://doi.org/10.4208/aamm.OA-2016-0115 Published online by Cambridge University Press

functional responses, impulsive effects, time delays and stage-structures (see, for example, [16,22,23,28,32,52,56,63]) and obtained some results on permanence, global existence of solution, asymptotic stability, or instability of the nontrivial states and periodicity of solutions. In the present paper, we extension to the study of population dynamics from two species predator-prey model to a three species space fractional reaction-diffusion systems consisting of two preys and one predator with impulsive effect.

Many ecological processes are governed by the fact that they experience a sudden change of state at certain moment of time. These processes evolve as a result of short-time perturbation with a very small time-lag in comparison with the period of the process. In natural sense, it is reasonable to assume that perturbation arise in the form of impulse, and most biological phenomena involving pharmacokinetics systems, thresholds and optimal control models exhibit some kind of impulsive effects. Various work has been done where impulsive control strategy is utilized to investigate the behaviour of the predator-prey dynamics, see [34, 53, 57, 58, 61, 62, 64] and references therein.

The ecological implication of the systems involve three species **U**, **V** and **W**, where **W** is the predator that feeds on both preys **U** and **V**. This type of ecological systems best describe the spatial interactions between the prey and predators among many biological species. Let $u(x,t)$, $v(x,t)$ and $w(x,t)$ be the corresponding scaled density functions of **U**, **V** and **W**, respectively at position x and time t. Then the ecological equations governing their density functions are given in the form of Lotka-Volterra type which consist of two preys and one predator with impulsive effect. A coupled fractional reaction-diffusion system of n $(n \leq 3, n \text{ integer})$ species which interact in a nonlinear fashion and diffuse may be modelled by the equations

$$u_t - D_1\Delta^{\eta/2}u = f(u,v,w), \tag{1.1a}$$
$$v_t - D_2\Delta^{\eta/2}v = g(u,v,w) \quad \text{in } \Omega\times[0,\infty), \quad t\neq T(\epsilon), \tag{1.1b}$$
$$w_t - D_3\Delta^{\eta/2}w = h(u,v,w), \tag{1.1c}$$
$$B[u] = B[v] = 0, \quad B[w] = \mathcal{S} \quad \text{on } \partial\Omega\times[0,\infty), \quad t = T(\epsilon), \tag{1.1d}$$
$$u(x,0) = u_0(x), \quad v(x,0) = v_0(x), \quad u(x,0) = u_0(x), \quad (x,t)\in\Omega, \tag{1.1e}$$

where the local kinetics are given as

$$f(u,v,w) = \tau_1 u\left(1-\frac{u}{\kappa_1}\right) - \frac{\alpha_1\varphi_1 uw}{\beta_1+u+\gamma_1 w}, \tag{1.2a}$$
$$g(u,v,w) = \tau_2 v\left(1-\frac{v}{\kappa_2}\right) - \frac{\alpha_2\varphi_2 vw}{\beta_2+v+\gamma_2 w}, \tag{1.2b}$$
$$h(u,v,w) = \left(\frac{\rho_1\alpha_1 u}{\beta_1+u+\gamma_1 w} - \psi_1\right)\varphi_1 w + \left(\frac{\rho_2\alpha_2 v}{\beta_2+v+\gamma_2 w} - \psi_2\right)\varphi_2 w, \tag{1.2c}$$

and Δ denotes the Laplacian operator in one, two or more dimensional space, $\Delta^{\eta/2}$ stands

https://doi.org/10.4208/aamm.OA-2016-0115 Published online by Cambridge University Press

for the Riemann-Liouville fractional integration of order η given as

$$\Delta^{\eta/2}=\frac{1}{\Gamma(\eta/2)}\int_0^x (x-\xi)^{\frac{\eta}{2}-1}\mathcal{F}(\xi)d\xi, \quad \eta>0, \quad x>0,$$

in the superdiffusive interval $1<\eta<2$. The Ω is a bounded region in $\mathbf{R}^3_+$ with boundary $\partial\Omega$. The diffusion coefficients D_i $(i=1,2,3)$, the intrinsic growth rates τ_i $(i=1,2)$ and the cropping rate α_i $(i=1,2)$ are all positive parameters, the carrying capacity of the preys $(\mathbf{U},\mathbf{V})$ κ_i, the saturation constants β_i, the predator interference γ_i, predator death rates ψ_i in patch i, and φ_i which represents the segment of lifetime an average predator waits in patch i, the rate, at which resources are converted to a new consumers is denoted by ρ_i, for $i=1,2$ are all nonnegative constants, and we also assume that the initial functions u_0, v_0 and w_0 are all nonnegative constants. Period of the impulsive effect is denoted by T, $\epsilon\in N$, N is a set of positive integers [58,61,64], $\mathcal{S}>0$ is the amount release by predator $\mathbf{W}$ at $t=T(\epsilon)$.

Fractional calculus is considered as a subject of considerable interest in the fields of applied engineering, mathematics and physics, [7, 26, 27, 29, 55, 60]. Nowadays, fractional derivatives has gained a significant development to model some real life phenomena in the form of partial differential equations or the ordinary equation. Most physical problems are modeled mathematically in fractional form by replacing the second order partial derivative in classical reaction-diffusion equation with the fractional derivative of order η. Similar expression are given for the time fractional problems. Finding an accurate and reliable numerical method to numerically simulate this class of problem is another research work undertaken in this paper. Among several researchers that have studied the numerical simulation of fractional reaction diffusion problems include [1–4, 8, 10–12, 14, 39, 40, 47, 48] and references therein.

The aims of this paper are in folds: We begin by establishing the conditions that guarantee that model (1.1) is locally and globally asymptotically stable for the preys-species $(\mathbf{U},\mathbf{V})$ washout periodic solutions. Again, since the nature of system (1.1) permits splitting into fractional and reaction terms, we conveniently introduced two notable mathematical ideas for the stiff and moderately stiff parts. We formulate an efficient numerical method based on the exponential time differencing Adams scheme to advance the resulting system of ordinary differential equations arising from the approximation of fractional reaction-diffusion equation, when the Fourier spectral method is applied. By the numerical simulation, we examine the influences on the inherent oscillation caused by the impulsive perturbations in one, two and three spatial dimensions to indicate both ecological and numerical implications.

The rest of the paper is organized as follows. We present mathematical analysis of the main results which show that the model is both locally and asymptotically stable in Section 2. In Section 3, we formulate adaptive numerical methods for solving general space fractional reaction-diffusion equation. Applicability and suitability of the proposed method is examined in one and high dimensions in Section 4. We finally conclude the paper with Section 5.

https://doi.org/10.4208/aamm.OA-2016-0115 Published online by Cambridge University Press

2 Mathematical analysis

In the spirits of [6, 36], we examine the local stability analysis of (1.1). let $\mathbf{R}_+ = [0,\infty)$, $\mathbf{R}^3_+ = \{X \in \mathbf{R}^3 | X \geq 0\}$. We let $\mathcal{G} = (f(u,v,w), g(u,v,w), h(u,v,w))^{\mathrm{T}}$ as the map that defines the reaction terms. Let $\mathcal{H} : \mathbf{R}_+ \times \mathbf{R}^3_+ \to \mathbf{R}_+$, then $\mathcal{H} \in \mathcal{H}_0$ if; $\mathcal{H}$ is continuous in $(T(\epsilon), T(\epsilon+1)] \times \mathbf{R}^4_+$, for each $X \in \mathbf{R}^4_+$, $\epsilon \in N$,

$$\lim_{(t,\mathcal{Z})\to(T^+(\epsilon),X)} \mathcal{H}(t,\mathcal{Z}) = \mathcal{H}(T^+(\epsilon),X)$$

exists. And, $\mathcal{H}$ is said to be locally Lipschitzian in X. The local stability analysis is examined in order to see behaviour of the local dynamics in the absence of diffusive terms, that is, when $D_i = 0$, $i = 1,2,3$. The steady states of system (1.1) are determined by setting the local kinetic terms $f(u,v,w) = g(u,v,w) = h(u,v,w) = 0$.

Definition 2.1. Suppose that function $\mathcal{G}(t) = (u(t), v(t), w(t))$ is smooth and satisfy (1.1) in $\mathbf{R}^3_+$, and every component of $\mathcal{G}$ is almost periodic function, we say that $\mathcal{G}$ is a spatial homogeneity periodic solution of (1.1) represented by $\mathcal{G}(t, T(\epsilon))$, for every $\epsilon > 0$.

Theorem 2.1. *Assume* (u,v,w) *to be any solution of model* (1.1)*, then the equilibrium point* $(0,0,\hat{w})$ *which corresponds to the extinction of preys species is locally asymptotically stable if*

$$\frac{\alpha_1\varphi_1}{\gamma_1(\psi_1\varphi_1+\psi_2\varphi_2)}\ln\left\{1-\frac{\gamma_1\mathcal{S}(1-\exp(-\psi_1\varphi_1T-\psi_2\varphi_2T))}{\gamma_1\mathcal{S}+\beta_1(1-\exp(-\psi_1\varphi_1T-\psi_2\varphi_2T))}\right\}+\tau_1T<0, \tag{2.1}$$

and

$$\frac{\alpha_2\varphi_2}{\gamma_2(\psi_1\varphi_1+\psi_2\varphi_2)}\ln\left\{1-\frac{\gamma_2\mathcal{S}(1-\exp(-\psi_1\varphi_1T-\psi_2\varphi_2T))}{\gamma_1\mathcal{S}+\beta_2(1-\exp(-\psi_1\varphi_1T-\psi_2\varphi_2T))}\right\}+\tau_2T<0. \tag{2.2}$$

Proof. We can determine the local stability of prey eradication periodic solution $(0,0,\hat{w})$ by examining the behaviour of system (1.1) subject to small amplitude perturbation

$$(u,v,w) = (\bar{u},\bar{v},\bar{w}+\hat{w}). \tag{2.3}$$

Using (2.3) in (1.1), we have the linearized system written in the form

$$\frac{d\bar{u}}{dt} = \bar{u}\left(\tau_1 - \frac{\alpha_1\varphi_1\hat{w}}{\beta_1+\gamma_1\hat{w}}\right), \tag{2.4a}$$

$$\frac{d\bar{v}}{dt} = \bar{v}\left(\tau_2 - \frac{\alpha_2\varphi_2\hat{w}}{\beta_2+\gamma_2\hat{w}}\right), \quad t \neq T(\epsilon), \tag{2.4b}$$

$$\frac{d\bar{w}}{dt} = \bar{w}(-\psi_1\varphi_1 - \psi_2\varphi_2), \tag{2.4c}$$

$$B[\bar{u}] = B[\bar{v}] = B[\bar{w}] = 0, \quad t = T(\epsilon), \tag{2.4d}$$

https://doi.org/10.4208/aamm.OA-2016-0115 Published online by Cambridge University Press

which leads to

$$(\bar{u},\bar{v},\bar{u})^{\mathbf{T}}=\mathbf{A}(\bar{u}(0),\bar{v}(0),\bar{w}(0))^{\mathbf{T}},\quad 0\leq t\leq T,$$

where $\mathbf{A}$ at point $(\bar{u}(0),\bar{v}(0),\bar{w}(0))$ satisfies

$$\frac{d\mathbf{A}}{dt}=\begin{pmatrix}\tau_1-a & 0 & 0\\ 0 & \tau_2-b & 0\\ 0 & 0 & -c\end{pmatrix}\mathbf{A}(t), \tag{2.5}$$

with

$$a=\frac{\alpha_1\varphi_1\hat{w}}{\beta_1+\gamma_1\hat{w}},\quad b=\frac{\alpha_2\varphi_2\hat{w}}{\beta_2+\gamma_2\hat{w}},\quad c=\psi_1\varphi_1+\psi_2\varphi_2,\quad \mathbf{A}(0)=\mathbf{I},$$

is the identity matrix, and

$$[(\bar{u};\bar{v};\bar{w})T^{+}(\epsilon)]=[1,0,0;0,1,0;0,0,1][(\bar{u};\bar{v};\bar{w})T(\epsilon)].$$

So, stability of the periodic prey extinction at point $(0,0,\hat{w})$ can be examined by the eigenvalues of $[1,0,0;0,1,0;0,0,1]\mathbf{A}(T)$, which have an absolute value of less than one. Then, the state $(0,0,\hat{w})$ is locally stable. Based on Floquet theory, all the eigenvalues

$$\lambda_1=\exp\left(\int_0^T(\tau_1-a)\right),\quad \lambda_2=\exp\left(\int_0^T(\tau_2-b)\right),\quad \lambda_3=\exp(-c(T))<1.$$

Hence, the point $(0,0,\hat{w})$ is locally asymptotically stable if $|\lambda_1|<1$ and $|\lambda_2|<1$, which imply that conditions (2.1) and (2.2) are satisfied. The proof is completed. □

Definition 2.2. For any positive smooth initial data $\mathcal{G}(x,0)=(u(x,0),v(x,0),w(x,0))=(u_0(x),v_0(x),w_0(x))\geq 0$, $\mathcal{G}(x,0)\neq 0$, $x\in\Omega$, if there exist a unique nonnegative solution $\mathcal{G}(x,t)=(u(x,t),v(x,t),w(x,t))$ for the model (1.1), subject to the boundary conditions, and

$$\lim_{t\to\infty}(\mathcal{G}_{(u,v,w)}(x,t)-\mathcal{G}_{(u,v,w)}(t,T(\epsilon)))$$

uniformly for all $x\in\Omega$, we say that spatial homogeneity periodic solution $\mathcal{G}(t,T(\epsilon))$ is globally asymptotically stable.

Definition 2.3. Predator-prey system (1.1) is said be permanent if there exists a compact $\Omega\subset\mathbf{R}^3_+$ such that every solution $(u(x,t),v(x,t),w(x,t))$ of the given system (1.1) exist mainly, and remain bounded in the region of definition Ω.

Theorem 2.2. *If (u,v,w) is the solution of* (1.1)*, then the point $(0,0,\hat{w})$ which represents the prey species extinction is said to be globally asymptotically stable if*

$$\frac{\alpha_1\varphi_1}{\gamma_1(\psi_1\varphi_1+\psi_2\varphi_2)}\ln\left\{1-\frac{\gamma_1\mathcal{S}(1-\exp(-\psi_1\varphi_1T-\psi_2\varphi_2T))}{\gamma_1\mathcal{S}+\beta_1(1-\exp(-\psi_1\varphi_1T-\psi_2\varphi_2T))}\right\}+\tau_1T<0, \tag{2.6a}$$

$$\frac{\alpha_2\varphi_2}{\gamma_2(\psi_1\varphi_1+\psi_2\varphi_2)}\ln\left\{1-\frac{\gamma_2\mathcal{S}(1-\exp(-\psi_1\varphi_1T-\psi_2\varphi_2T))}{\gamma_1\mathcal{S}+\beta_2(1-\exp(-\psi_1\varphi_1T-\psi_2\varphi_2T))}\right\}+\tau_2T<0, \tag{2.6b}$$

https://doi.org/10.4208/aamm.OA-2016-0115 Published online by Cambridge University Press

and

$$\mathcal{S}\geq\max\left\{\frac{\gamma_1(\psi_1\varphi_1+\psi_2\varphi_2)T(\beta_1+\mathcal{J}+\gamma_1\mathcal{J})}{\alpha_1\varphi_1},\frac{\gamma_2(\psi_1\varphi_1+\psi_2\varphi_2)T(\beta_2+\mathcal{J}+\gamma_2\mathcal{J})}{\alpha_2\varphi_2}\right\}.$$

For a positive constant $\mathcal{J}$, we have $u\leq\mathcal{J},v\leq\mathcal{J},w\leq\mathcal{J}$ for each solution $X=(u,v,w)$ of ecological model (1.1)*, for t large.*

Proof. Let $\mathcal{H}=\kappa_1u+\kappa_2v$, from (1.1) in absence of diffusion, we obtain

$$\mathcal{H}'=\kappa_1\tau_1u-\tau_1u^2-\frac{\alpha_1\kappa_1\varphi_1uw}{u+\gamma_1w+\beta_1}+\kappa_2\tau_2v-\tau_2v^2-\frac{\alpha_2\kappa_2\varphi_2vw}{v+\gamma_2w+\beta_2}.$$

Also, we let a constant $\mathcal{Q}>0$ in such a way that $u,v,w\leq\mathcal{Q}$ for any solution (u,v,w) of system (1.1) with all $t>0$ and large enough. Then,

$$\mathcal{H}'\leq\kappa_1\tau_1u-\tau_1u-\frac{\alpha_1\kappa_1\varphi_1uw}{\mathcal{Q}+\gamma_1\mathcal{Q}+\beta_1}+\kappa_2\tau_2v-\tau_2v-\frac{\alpha_2\kappa_2\varphi_2vw}{\mathcal{Q}+\gamma_2\mathcal{Q}+\beta_2},$$

which yields

$$\begin{aligned}w'&=\left(\frac{\alpha_1\rho_1u}{u+\gamma_1w+\beta_1}-\psi_1\right)\varphi_1w+\left(\frac{\alpha_2\rho_2v}{v+\gamma_2w+\beta_1}-\psi_2\right)\varphi_2w\\&\geq-w(\psi_1\varphi_1+\psi_2\varphi_2),\quad t\neq T(\epsilon),\\B[w]&=\mathcal{S},\quad t=T(\epsilon).\end{aligned}$$

In the solution, there exists a $t_1>0$, and a small positive constant, say δ, in such a way that $w\geq\hat{w}-\delta$, valid for all $t\geq t_1$. We have

$$w\geq\frac{\mathcal{S}\exp(-(\psi_1\varphi_1+\psi_2\varphi_2)T)}{1-\exp(-(\psi_1\varphi_1+\psi_2\varphi_2)T)}-\delta$$

and

$$\mathcal{H}'\leq\left(\kappa_1\tau_1-\frac{\alpha_1\kappa_1\varphi_1\Gamma}{\mathcal{Q}+\gamma_1\mathcal{Q}+\beta_1}\right)u+\left(\kappa_2\tau_2-\frac{\alpha_2\kappa_2\varphi_2\Gamma}{\mathcal{Q}+\gamma_2\mathcal{Q}+\beta_2}\right)v,$$

where

$$\Gamma\equiv\frac{\mathcal{S}\exp(-(\psi_1\varphi_1+\psi_2\varphi_2)T)}{1-\exp(-(\psi_1\varphi_1+\psi_2\varphi_2)T)}-\delta.$$

For

$$\kappa_1\tau_1-\frac{\alpha_1\kappa_1\varphi_1\Gamma}{\mathcal{Q}+\gamma_1\mathcal{Q}+\beta_1}<0\quad\text{and}\quad\kappa_2\tau_2-\frac{\alpha_2\kappa_2\varphi_2\Gamma}{\mathcal{Q}+\gamma_2\mathcal{Q}+\beta_2}<0,$$

then we can say that

$$\mathcal{S}\geq\max\left\{\frac{\tau_1(\psi_1\varphi_1+\psi_2\varphi_2)T}{\alpha_1\varphi_1}(\gamma_1\mathcal{Q}+\beta_1),\frac{\tau_2(\psi_1\varphi_1+\psi_2\varphi_2)T}{\alpha_2\varphi_2}(\gamma_2\mathcal{Q}+\beta_2)\right\}.$$

https://doi.org/10.4208/aamm.OA-2016-0115 Published online by Cambridge University Press

For $t>t_1$, we have

$$\mathcal{H}' \leq \left(\kappa_1\tau_1 - \frac{\alpha_1\kappa_1\varphi_1\Gamma}{\mathcal{Q}+\gamma_1\mathcal{Q}+\beta_1}\right)u + \left(\kappa_2\tau_2 - \frac{\alpha_2\kappa_2\varphi_2\Gamma}{\mathcal{Q}+\gamma_2\mathcal{Q}+\beta_2}\right)v < 0$$

as $\mathcal{H}\to 0$, so also $u,v\to 0$ for $t\to\infty$. Hence, we conclude that the model (1.1) is globally asymptotically stable for the prey-species eradication state $(0,0,\hat{w})$. □

Theorem 2.3. *System* (1.1) *is said to be permanent if*

$$\frac{\alpha_1\varphi_1}{\gamma_1(\psi_1\varphi_1+\psi_2\varphi_2)}\ln\left\{1-\frac{\gamma_1\mathcal{S}(1-\exp(-\psi_1\varphi_1T-\psi_2\varphi_2T))}{\gamma_1\mathcal{S}+\beta_1(1-\exp(-\psi_1\varphi_1T-\psi_2\varphi_2T))}\right\}+\tau_1T>0, \tag{2.7a}$$

$$\frac{\alpha_2\varphi_2}{\gamma_2(\psi_1\varphi_1+\psi_2\varphi_2)}\ln\left\{1-\frac{\gamma_2\mathcal{S}(1-\exp(-\psi_1\varphi_1T-\psi_2\varphi_2T))}{\gamma_1\mathcal{S}+\beta_2(1-\exp(-\psi_1\varphi_1T-\psi_2\varphi_2T))}\right\}+\tau_2T>0, \tag{2.7b}$$

and

$$\mathcal{S}<\max\left\{\frac{\gamma_1(\psi_1\varphi_1+\psi_2\varphi_2)T(\beta_1+\mathcal{J}+\gamma_1\mathcal{J})}{\alpha_1\varphi_1},\frac{\gamma_2(\psi_1\varphi_1+\psi_2\varphi_2)T(\beta_2+\mathcal{J}+\gamma_2\mathcal{J})}{\alpha_2\varphi_2}\right\}.$$

Proof. Let $\mathcal{G}(t)=(u(t),v(t),w(t)$ be the solution of the model (1.1) with $\mathcal{G}>0$. We also assume that $u(t)\leq\mathcal{J},v(t)\leq\mathcal{J}$ and $w(t)\leq\mathcal{J}$ with $t\geq 0$, where $\mathcal{J}$ is any nonnegative constant. By considering a subsystem of the form

$$\frac{dw(t)}{dt}=(\psi_1\varphi_1+\psi_2\varphi_2)w(t),\quad t\neq T(\epsilon),\quad w(t^+)=w(t)+\mathcal{J},\quad t=T(\epsilon),\quad w(0^+)=w_0.$$

We have $w(t)>\hat{w}(t)-e$ for all large t and

$$w(t)\geq\frac{\mathcal{S}\exp(-(\psi_1\varphi_1+\psi_2\varphi_2)T)}{1-\exp(-(\psi_1\varphi_1+\psi_2\varphi_2)T)}-e\triangleq\xi_1$$

for large t. Next, we obtain ξ_2, ξ_3 for $u(t)>\xi_2$ and $v(t)>\xi_3$.

Let e_1 be small positive number such that

$$\varrho_1\triangleq\exp\left(\int_{T(\epsilon)}^{T(\epsilon+1)}\left(\tau_1\left(1-\frac{\mathcal{J}}{\kappa_1}\right)-\frac{\alpha_1\varphi_1(v_3^*+e_1)}{\beta_1}\right)dt\right)>1.$$

We will now show that there exists ξ_2, such that $u(t)\geq\xi_2$ for large t. Also, we will show there exists a $t_1\in(0,\infty)$ such that $u(t)\geq\xi_2$. Else, $u(t)<\xi_2$, $\forall t>0$. From model (1.1), one gets

$$\frac{dw(t)}{dt}\leq\left(\frac{\rho_1\alpha_1\varphi_1\xi_2}{\beta_1}+\frac{\rho_2\alpha_2\varphi_2\mathcal{J}}{\beta_2}-(\psi_1\varphi_1+\psi_2\varphi_2)\right)w(t),\quad t\neq T(\epsilon), \tag{2.8a}$$

$$w(t^+)=w(t)+\mathcal{J},\quad t=T(\epsilon),\quad w(0^+)=w_0. \tag{2.8b}$$

https://doi.org/10.4208/aamm.OA-2016-0115 Published online by Cambridge University Press

Thus, we get $w(t)\leq v_3$ and $v_3\to v_3^*$, as $t\to\infty$, where v_3 is regarded as the solution of

$$\frac{dv_3(t)}{dt}\leq\left(\frac{\rho_1\alpha_1\varphi_1\xi_2}{\beta_1}+\frac{\rho_2\alpha_2\varphi_2\mathcal{J}}{\beta_2}-(\psi_1\varphi_1+\psi_2\varphi_2)\right)v_3(t),\quad t\neq T(\epsilon), \tag{2.9a}$$

$$v_3(t^+)=v_3(t)+\mathcal{J},\quad t=T(\epsilon),\quad v_3(0^+)=v_0, \tag{2.9b}$$

and

$$v_3^*=\frac{\mathcal{S}\exp\left(-\left((\psi_1\varphi_1+\psi_2\varphi_2)-\frac{\rho_1\alpha_1\varphi_1\xi_2}{\beta_1}+\frac{\rho_2\alpha_2\varphi_2\mathcal{J}}{\beta_2}\right)(t-T(\epsilon))\right)}{1-\exp(-(\psi_1\varphi_1+\psi_2\varphi_2)T)},$$
$$t\in(T(\epsilon),T(\epsilon+1)],\quad \epsilon\in N.$$

Thus, there exists a $T_1>0$ such that

$$w(t)\leq_3(t)<v_3^*+e_1$$

and

$$\frac{du(t)}{dt}\geq u(t)\left[\tau_1\left(1-\frac{\mathcal{J}}{\kappa_1}\right)-\frac{\alpha_1\varphi_1(v_3^*+e_1)}{\beta_1}\right]. \tag{2.10}$$

Assume $N_1\in N$ and $N_1T\geq T_2>T_1$, by integrating Eq. (2.10) on time interval $(T(\epsilon),T(\epsilon+1))$, $n\geq N_1$, we obtain

$$\begin{aligned}u(T(\epsilon+1))&\geq u(T^+(\epsilon))\exp\left(\int_{T(\epsilon)}^{T(\epsilon+1)}\left(\tau_1\left(1-\frac{\mathcal{J}}{\kappa_1}\right)-\frac{\alpha_1\varphi_1(v_3^*+e_1)}{\beta_1}\right)dt\right)\\&=u(T(\epsilon))\exp\left(\int_{T(\epsilon)}^{T(\epsilon+1)}\left(\tau_1\left(1-\frac{\mathcal{J}}{\kappa_1}\right)-\frac{\alpha_1\varphi_1(v_3^*+e_1)}{\beta_1}\right)dt\right)\\&=u(T(\epsilon))\varrho_1.\end{aligned}$$

Then for $u((N_1+\tau)T)\geq u(N_1T)\varrho_1^\kappa\to\infty$, and $\kappa\to\infty$, there exists a contradiction to the boundedness of $u(t)$, for t_1, such that $u(t_1)\geq\xi_2$.

Secondly, if $u(t)\geq\xi_2$ for all $t\geq t_1$, then our aim is achieved. Thus we only require to consider the solution in the given region $R=\{u(t):u(t)<\xi_2\}$. Assume $\hat{t}=\inf_{t\geq t_1}$, then $u(t)\geq\xi_2$, $t\in(t,\hat{t})$ and $\hat{t}\in(T(\epsilon),T(\epsilon+1)$, $\epsilon_1\in N$. It is convenient to show that $u(\hat{t})=\xi_2$ since $u(t)$ is continuous. Here we let $t_2\in(T(\epsilon_1+1),T(\epsilon_1+1)+\hat{T})$ such that $u(t_2)\geq\xi_2$, or else $u(t)<\xi_2$, $t\in(T(\epsilon_1+1),T(\epsilon_1+1)+\hat{T})$, $\hat{T}=T(\epsilon_2+T(\epsilon_3))$. By letting $\epsilon_2,\epsilon_3\in N$ in such that

$$T(\epsilon_2-1)>\frac{\ln\left(\frac{e_1}{(\mathcal{J}+\mathcal{S})}\right)\exp(\omega(\epsilon_2+1)T)\varrho_1^{\epsilon_3}}{\frac{\rho_1\alpha_1\varphi_1\xi_2}{\beta_1}+\frac{\rho_2\alpha_2\varphi_2\mathcal{J}}{\beta_2}-(\psi_1\varphi_1+\psi_2\varphi_2)}>1.$$

we now consider Eq. (2.9) with $v_3(\hat{t}^+)=w(\hat{t}^+)$, to obtain

$$\begin{aligned}v_3(t)=&\left[v(T^+(\epsilon_1+1))-\frac{\mathcal{S}}{1-\exp\left(\frac{\rho_1\alpha_1\varphi_1\xi_2}{\beta_2}T+\frac{\rho_2\alpha_2\varphi_2\mathcal{J}}{\beta_2}T-(\psi_1\varphi_1+\psi_2\varphi_2)T\right)}\right]\\&\times\exp\left(\frac{\rho_1\alpha_1\varphi_1\xi_2}{\beta_1}t+\frac{\rho_2\alpha_2\varphi_2\mathcal{J}}{\beta_2}t-(\psi_1\varphi_1+\psi_2\varphi_2)t\right)+v_3^*(t)\end{aligned}$$

https://doi.org/10.4208/aamm.OA-2016-0115 Published online by Cambridge University Press

for $t\in(t(\epsilon),T(\epsilon+1),\epsilon_1+1<\epsilon<\epsilon_1+\epsilon_2+\epsilon_3+1)$, then

$$\begin{aligned}&|vv_3(t)-v_3^*(t)|\\&<(\mathcal{J}+\mathcal{S})\exp\left(-\left((\psi_1\varphi_1+\psi_2\varphi_2)-\frac{\rho_1\alpha_1\varphi_1\xi_2}{\beta_1}-\frac{\rho_2\alpha_2\varphi_2\mathcal{J}}{\beta_2}\right)(t-T(\epsilon_1+1))\right)\\&<e_1\end{aligned}$$

and

$$w(t)\leq v_3(t)\leq v_3^*(t)+e_1,T(\epsilon_1+\epsilon_2+1)\leq t\leq T(\epsilon_1+1)\hat{T},$$

which justifies that Eq. (2.10) is true for $T(\epsilon_1+\epsilon_2+1)\leq t\leq T(\epsilon_1+1)+\hat{T}$. By integrating (2.10) on $T(\epsilon_1+\epsilon_2+1),T(\epsilon_1+1)+\hat{T}$ we get

$$u(T(\epsilon_1+\epsilon_2+\epsilon_3+1))\geq u(T(\epsilon_1+\epsilon_2+1))\varrho_1^{\epsilon_3}.$$

There emerged two possible cases for $t\in(\hat{t},T(\epsilon_1+1))$.

Firstly, if $u(t)<\xi_2$ for all $t\in(\hat{t},T(\epsilon_1+1))$, then $u(t)<\xi_2$ for all $t\in(\hat{t},T(\epsilon_1+\epsilon_2+1))$, so that

$$\frac{du(t)}{dt}\geq u(t)\left[\tau_1\left(1-\frac{\xi_2}{\kappa_1}\right)-\frac{\alpha_1\varphi_1\mathcal{J}}{\beta_1}\right]=\omega u(t). \tag{2.11}$$

By integrating the above equation on $(\hat{t},T(\epsilon_1+\epsilon_2+1))$, which results in

$$u(T(\epsilon_1+\epsilon_2+1))\geq u(\hat{t})\exp(\omega T(\epsilon_2+1)).$$

Then

$$u(T(\epsilon_1+\epsilon_2+\epsilon_3+1))\geq\xi_2\exp(\omega T(\epsilon_2+1))\varrho_1^{\epsilon_3}>\xi_2,$$

which lead to a contradiction.

Let $t_3=\inf_{t>\hat{t}}\{u(t)\geq\xi_2\}$, then $u(t_3)=\xi_2$ and Eq. (2.11) is true for $t\in[\hat{t},t_3)$. If we integrate (2.11) on $[\hat{t},t_3)$ we have

$$u(t)\geq u(\hat{t})\exp(\omega(t-\hat{t}))\geq\xi_2\exp(\omega T(\epsilon_1+\epsilon_2+\epsilon_3+1))\triangleq\hat{\xi}_2.$$

So for $t>t_3$, we continue with the same argument since $u(t_3)\geq\xi_2$. Hence we can conclude that $u(t)\geq\hat{\xi}_2$ for $t>t_3$.

Secondly, let there exists $t_m\in(\hat{t},T(\epsilon_1+1)]$ such that $u(t_m)\geq\xi_2$. Assume $t_k=\inf_{t>\hat{t}}\{u(t)\geq\xi_2\}$, then $u(t)<\xi_2$ for all $t\in[\hat{t},t_4)$ and $u(t_k)=\xi_2$. For $t\in[\hat{t},t_k)$, Eq. (2.11) is true on $[\hat{t},t_k)$, we have $u(t)\geq u(\hat{t})\exp(\omega(t-\hat{t}))>\xi_2$. The process is continuous as long as $u(t_k)\geq\xi_2$. And we have $u(t)\geq\xi_2$ for all $t>t_k$. Hence, we conclude in both cases that $u(t)\geq\xi_2$ for all $t\geq t_1$. Similar prove holds for $v(t)\geq\hat{\xi}_3$ for all $t\geq t_2$. Knowing well that the set $\Omega\in\mathbf{R}_+^3$ is global attractors, the solution of model (1.1) enters and remain in Ω, which shows that the model is permanent. □

https://doi.org/10.4208/aamm.OA-2016-0115 Published online by Cambridge University Press

3 Numerical methods

Spectral methods have been considered as the logical extension of conventional finite differences to infinite order [9,14,19,24], due to its ability to remove the issue stiffness that is inherent with the diffusive term of fractional reaction-diffusion equations [42, 54, 59]. Based on the known integrating factor technique, we shall formulate the theory here in one spatial dimension.

In a compact form, system (1.1) can be written as

$$u_t = D_1\Delta^{\eta/2}u + f(u,v,w), \quad v_t = D_2\Delta^{\eta/2}v + g(u,v,w), \quad w_t = D_3\Delta^{\eta/2}w + h(u,v,w), \tag{3.1}$$

where $f(u,v,w)$, $g(u,v,w)$ and $h(u,v,w)$ are nonlinear term functions of u, v and w, D_i, 1, 2, 3 are the respective diffusion coefficients of species $u(x,t)$, $v(x,t)$ and $w(x,t)$ in the spatial direction x and time t. The solution of (3.1) is subject to the initial condition

$$u(x,0) = u_0(x), \quad v(x,0) = v_0(x), \quad w(x,0) = w_0(x), \tag{3.2}$$

and any of the boundary conditions:

- In the case of an infinite system, $x \in (-\infty,\infty)$, here $\mathbf{R}$ is a subset of $(-\infty,\infty)$.
- $x \in [0,L]$, $\frac{\partial u}{\partial x}(0,t) = \frac{\partial u}{\partial x}(L,t) = 0$, no-flux or Neumann boundary condition for a finite system, and
- $x \in [0,L]$, $\mathbf{u}(0,t) = \mathbf{u}(L,t) = \mathbf{u}_a$, called the Dirichlet or fixed concentration boundary condition, also for a fixed system.

By adopting the integrating factor technique to the Fourier transform of system (3.1) see, for instance (see [13,35,45,48]), we obtain

$$U_t(\chi_x,t) = D_1(\chi_x^{\eta/2})U(\chi_x,t) + \mathcal{F}[f(u(x,t),v(x,t),w(x,t))], \tag{3.3}$$

where U,V and W are the double Fourier transforms of species densities $u(x,t)$, with similar expressions for $V_t(\chi_x,t)$ and $W_t(\chi_x,t)$. In other words,

$$\mathcal{F}[u(x,t)] = U(\chi_x,t) = \int_{-\infty}^{\infty} u(x,t)e^{-i(\chi_x x)}dx. \tag{3.4}$$

To explicitly remove the inherent stiffness in the fractional partial derivative parts, we let $\Omega^{\eta/2} = \chi_x^{\eta/2}$, and set

$$U = e^{D_1\Omega^{\eta/2}t}\bar{U},$$

so that

$$\partial_t\bar{U} = e^{D_1\Omega^{\eta/2}t}\mathcal{F}[f(u,v,w)]. \tag{3.5}$$

https://doi.org/10.4208/aamm.OA-2016-0115 Published online by Cambridge University Press

In case of two spatial dimensions, one requires to discretize the square domain by considering the equispaced number of points N_x and N_y in the spatial directions of x and y. We employ the discrete fast Fourier transform (DFFT) [54] to transform Eq. (3.5) to a system of ODEs

$$\partial_t \bar{U}_{i,j} = e^{D_1 \Omega_{i,j}^{\eta/2} t} \mathcal{F}[f(u_{i,j}, v_{i,j}, w_{i,j})], \tag{3.6}$$

where $u_{i,j} = u(x_i, y_j)$ and $\Omega_{i,j}^{\eta/2} = \chi_x^{\eta/2}(i) + \chi_y^{\eta/2}(j)$. Boundary conditions are now set at extremes of the domain of size L^2 or $\pm L$ depending on the choice of boundary conditions. In the 2D experiment, we use a square Fourier nodes of size $L \times L$ for $N_x = N_y = N = L$. At this stage, the system has been converted to ODEs, the stiffness issue is far gone. It should be noted that any explicit higher-order time stepping methods can be used, and the formulation here can be extended to any higher dimensional space for a multi-species system. So once the stiffness is removed, one can advance in time with any higher order time solver, see [17, 20, 35, 42, 43, 49] for details. In what follows, we discuss the formulation of exponential time differencing method of Adams-type.

3.1 Exponential Adams-type schemes

The main idea behind the exponential time differencing schemes is to construct integrators [30,31] of multistep type through variation of parameters between t_n and $t_{n+1}=t_n+h$. We obtain

$$\begin{aligned} \omega(t_{n+1}) &= e^{\mathbf{L}h}\omega(t_n) + e^{t_n \mathbf{L}} \int_{t_n}^{t_n+h} e^{-\tau \mathbf{L}} \mathbf{N}(\tau, \omega(\tau)) d\tau \\ &= e^{\mathbf{L}h}\omega(t_n) + \int_0^h e^{(h-\tau)\mathbf{L}} \mathbf{N}(t_n+\tau, \omega(t_n+\tau)) d\tau. \end{aligned} \tag{3.7}$$

The derivation of the numerical method proceeds in the same way as in [17] for explicit Adams methods. Given that $\omega_j \approx \omega(t_j)$, we naturally define a new approximation $\omega_{n+1} \approx \omega(t_{n+1})$ given by

$$\omega_{n+1} = e^{\mathbf{L}h}\omega_n + \int_0^h e^{(h-\tau)\mathbf{L}} P_{n,k-1}(t_n+\tau) d\tau, \tag{3.8}$$

where $P_{n,k-1}$ is the Lagrange polynomial interpolated through the points

$$(t_{n-k+1}, \mathbf{N}(t_{n-k+1}, \omega_{n-k+1})), \cdots, (t_n, \mathbf{N}(t_n, \omega_n)),$$

and is given by

$$P_{n,k-1}(t_n+\theta h) = \sum_{j=0}^{k-1} (-1)^j \begin{pmatrix} -\theta \\ j \end{pmatrix} \nabla^j \mathbf{N}_j, \quad \mathbf{N}_j = \mathbf{N}(t_j, \omega_j). \tag{3.9}$$

https://doi.org/10.4208/aamm.OA-2016-0115 Published online by Cambridge University Press

Here, ∇ denotes the standard backward difference operator, given by

$$\nabla^0\mathbf{N}_n=\mathbf{N}_n,\quad \nabla^j\mathbf{N}_n=\nabla^{j-1}\mathbf{N}_n-\nabla^{j-1}\mathbf{N}_{n-1},\quad j=1,2,\cdots. \tag{3.10}$$

The substitution of the Lagrange interpolation polynomial (3.9) into (3.8) yields the following scheme

$$\omega_{n+1}=e^{\mathbf{L}h}\omega_n+h\sum_{j=0}^{k-1}\gamma_j(\mathbf{L}h)\nabla^j\mathbf{N}_n, \tag{3.11}$$

where

$$\gamma_j(z)=(-1)^j\int_0^1 e^{(1-\theta)z}\begin{pmatrix}-\theta\\ j\end{pmatrix}d\theta. \tag{3.12}$$

The weight function (3.12) can be represented in term of the φ-functions

$$\varphi_j(z)=\frac{1}{(j-1)!}\int_0^1 e^{(1-\theta)z}\theta^{j-1}d\theta,\quad j\geq 0. \tag{3.13}$$

As in [30], we can represent (3.11) as

$$\omega_{n+1}=e^{\mathbf{L}h}\omega_n+h\sum_{j=0}^{k}\bar{\beta}_j\mathbf{N}_{n-j}, \tag{3.14}$$

where the coefficients $\bar{\beta}_j$ are linear combinations of matrix weight functions φ_j.

The explicit $(\bar{\beta}_0=0)$ ETD Adams-Bashforth method of order 4 is given by

$$\begin{pmatrix}\bar{\beta}_1\\ \bar{\beta}_2\\ \bar{\beta}_3\\ \bar{\beta}_4\end{pmatrix}=\begin{pmatrix}1 & 11/6 & 2 & 1\\ 0 & -3 & -5 & -3\\ 0 & 3/2 & 4 & 3\\ 0 & -1/3 & -1 & -1\end{pmatrix}\begin{pmatrix}\varphi_1(\mathbf{L}h)\\ \varphi_2(\mathbf{L}h)\\ \varphi_3(\mathbf{L}h)\\ \varphi_4(\mathbf{L}h)\end{pmatrix}. \tag{3.15}$$

This method serves as the predictor. An implicit exponential Adams-Moulton method which may serve as corrector, is given by

$$\begin{pmatrix}\bar{\beta}_0\\ \bar{\beta}_1\\ \bar{\beta}_2\\ \bar{\beta}_3\end{pmatrix}=\begin{pmatrix}0 & 1/3 & 1 & 1\\ 1 & 1/2 & -2 & -3\\ 0 & -1 & 1 & 3\\ 0 & -1/6 & 0 & -1\end{pmatrix}\begin{pmatrix}\varphi_1(\mathbf{L}h)\\ \varphi_2(\mathbf{L}h)\\ \varphi_3(\mathbf{L}h)\\ \varphi_4(\mathbf{L}h)\end{pmatrix}. \tag{3.16}$$

The φ-functions described through (3.13) can be computed explicitly by a recursive formula

$$\left.\begin{aligned}&\varphi_0(z)=e^z,\\ &\varphi_j(z)=\frac{\varphi_{j-1}(z)-\varphi_{j-1}(0)}{z},\quad j\geq 1.\end{aligned}\right\} \tag{3.17}$$

https://doi.org/10.4208/aamm.OA-2016-0115 Published online by Cambridge University Press

Another way to compute the functions φ_j is to use the Taylor series representation. To this end we have for all complex numbers z, the representation

$$\varphi_j(z)=\sum_{k=j}^{\infty}\frac{1}{k!}z^{k-j}. \tag{3.18}$$

However, it is known that the computation of these functions in their explicit or Taylor series form suffers from computational inaccuracy for matrices whose eigenvalues approach to zero. This is generally the case when the spacial discretization is based on spectral methods. In order to overcome the numerical difficulties encountered in (3.17) and (3.18), we employ the Krylov projection algorithm [50]. The key idea behind this method, is to approximate the product of a matrix function $\varphi(A)$ (A is a $N\times N$ matrix) and a vector v using projection of the matrix and the vector onto the Krylov subspace $K_m(A,v)=span\{v,Av,\cdots,A^{m-1}v\}$. The orthonormal basis $\{v_1,v_2,\cdots,v_m\}$ of $K_m(A,v)$ is constructed using the modified Arnoldi iteration [5, 50] which can be written in matrix form as

$$AV_m=V_mH_m+\bar{h}_{m+1,m}v_{m+1}e_m^T, \tag{3.19}$$

where $\bar{h}_{m+1,m}$ is an entry of the Hessenberg matrix H_m, $e_m=(0,\cdots,0,1,0,\cdots,0)^T$ is the unit vector with 1 as the m^{th} coordinate, $\{v_1,v_2,\cdots,v_m,v_{m+1}\}$ is an orthonormal basis of $K_m(A,b)$, $V_m=[v_1v_2\cdots v_m]\in\mathbb{R}^{N\times m}$, and

$$H_m=V_m^TAV_m \tag{3.20}$$

is an upper Hessenberg matrix calculated as a side product of the iteration. Matrix $P=V_mV_m^T$ is a projector onto $K_m(A,v)$, thus $\varphi(A)v$ is approximated as a projection

$$\varphi(A)b\approx V_mV_m^T\varphi(A)V_mV_m^Tb. \tag{3.21}$$

Recalling (3.20) and observing that $v_1=v/\|v\|_2$ we make the final approximation through

$$\varphi(A)v\approx\|v\|_2V_m\varphi(H_m)e_1. \tag{3.22}$$

The advantage of this formulation is that H_m is a $m\times m$ matrix of smaller size $(m\ll N)$ and thus it is much cheaper to evaluate $\varphi(H_m)$ than $\varphi(A)$.

4 Numerical experiments

In this experiment, we present numerical simulation results of system (1.1) in one, two and three spatial dimensions. We first consider the non-diffusive form (1.1), to confirm if actually the theoretical and numerical findings are in agreement. Secondly, we now simulate the full fractional reaction-diffusion system at some instances of fractional power η in the superdiffusive scenarios.

https://doi.org/10.4208/aamm.OA-2016-0115 Published online by Cambridge University Press

4.1 A non-diffusive example

In order to ensure that our mathematical results corresponds to the numerical results, we first experiment the non-diffusive system (that is, $D_1=D_2=D_3=0$) with initial conditions and other parametric values chosen in the first quadrant to make our results biologically feasible for the prey eradication of system (1.1). With the set of parameters

$$\alpha_1=0.6,\quad \alpha_2=0.85,\quad \beta_1=1.52,\quad \beta_2=2.1,\quad \gamma_1=0.08,\quad \gamma_2=0.85, \tag{4.1a}$$

$$\tau_1=0.9,\quad \tau_2=1.2,\quad \kappa_1=18,\quad \kappa_2=15,\quad \rho_1=0.35,\quad \rho_2=0.45, \tag{4.1b}$$

$$\psi_1=0.16,\quad \psi_2=0.25,\quad \varphi_1=0.31,\quad \varphi_2=0.7, \tag{4.1c}$$

the condition for locally asymptotically stable in Theorem 2.1 is satisfied. It is noticeable in Fig. 1 that both preys u and v go to extinction. Hence, the theoretical result obtained in this paper is verified via a numerical solutions, since from Theorem 2.1 the solution $(0,0,\hat{w})$ is locally asymptotically stable. It is natural that in absence of prey which serves as food for the predator, the whole ecosystem will collapse. As depicted in panels (a)-(c), predator density is declining with increasing time t.

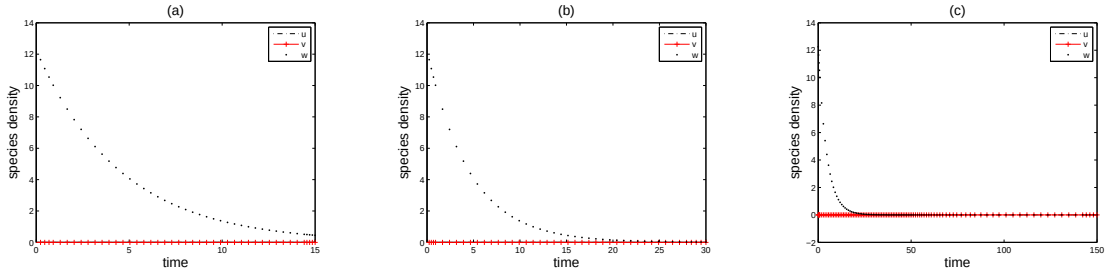


Figure 1: Time series of system (1.1) when $\mathcal{S}=4.5$. The numerical results depict preys u and v eradication at (a) $t=15$, (b) $t=30$ and (c) $t=150$. Other parameters as in (4.1).

With initial populations $u_0(x)=0.5$, $v_0(x)=0.33$ and $w_0(x)=0.2$, the numerical simulation of system (1.1) as displayed in Fig. 2 depicts a periodic solution in the presence of coexistence state of the species. The results in panels (b)-(d) are obtained with three initial values as shown in the figure legends.

4.2 One-dimensional example

In Fig. 3, we experiment the full fractional reaction-diffusion system (1.1) with kinetics (1.2) using the above parameters set (4.1), subject to zero-flux boundary conditions and initial populations given as

$$u(x,0)=0.53x+0.47\sin(-1.5\pi x), \tag{4.2a}$$

$$v(x,0)=1+\sin(2\pi x), \tag{4.2b}$$

$$w(x,0)=\hat{w}+10^{-8}(x-1200)(x-2800). \tag{4.2c}$$

https://doi.org/10.4208/aamm.OA-2016-0115 Published online by Cambridge University Press

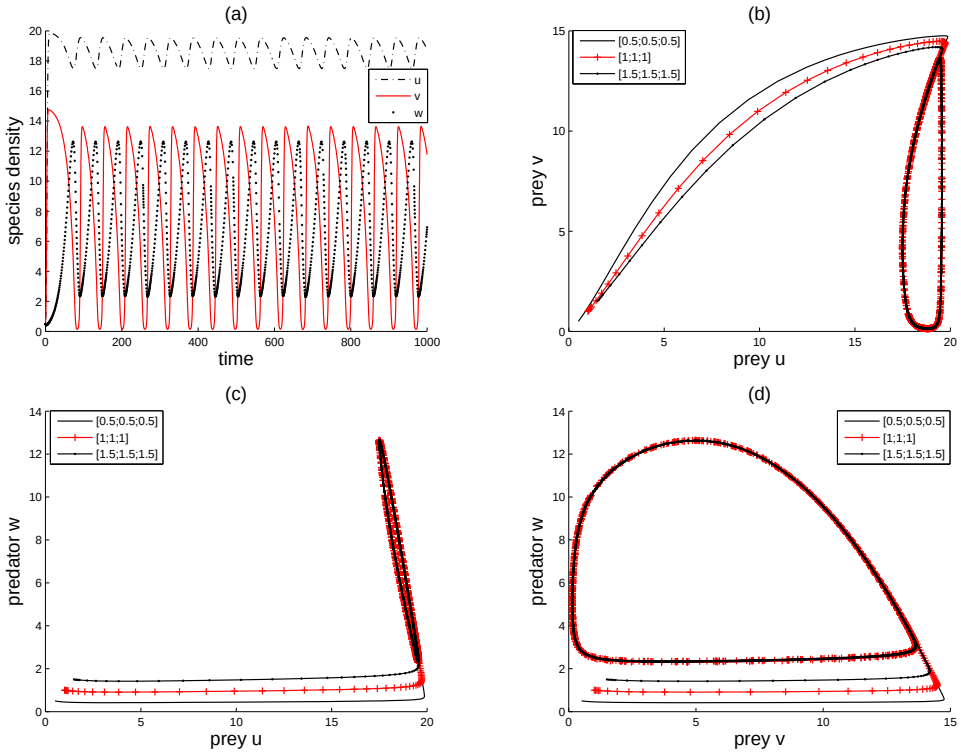


Figure 2: Coexistence of the species. panel (a) shows the periodic behaviour of the three species as a function of time. Panels (b)-(d) depict the limit cycles.

It is obvious that the three species exhibit various spatiotemporal oscillations in phase. Though depending of the choices of initial and parameter values, one can obtain distribution in which both preys u and v will evolve in similar fashion. The results displayed in Fig. 3 are obtained at time $t=30$ for two instances of fractional power η. The upper and lower plots correspond to $\eta=1.25$ and $\eta=1.75$ respectively.

We extend the suitability of the proposed numerical method in Fig. 4. Here, we examined the role of the cropping rates α_i, $i=1,2$ on the numerical results at different instances of time t and a fixed value of η for fractional reaction-diffusion system (1.1). In the simulations, we let $\alpha_1=4$ and $\alpha_2=3$ as against the previous values in Fig. 3 at various instants of final time $t=20,60,100,140$ for respective rows 1 to 4. We observed different chaotic and complex spatiotemporal oscillations. The three species, though coexist but oscillate in phase for all $t>0$. In our opinions, we strongly believed that these results have some biological interpretations. It should be mentioned that apart from the dynamical patterns displayed in this paper, other dynamical structures are obtainable depending on the choice of initial data and parameter values.

There is no exact solution for the predator-prey reaction-diffusion system (1.1). As a result, we numerically check the convergence of the ETD-ADAMS method by fixing the

https://doi.org/10.4208/aamm.OA-2016-0115 Published online by Cambridge University Press

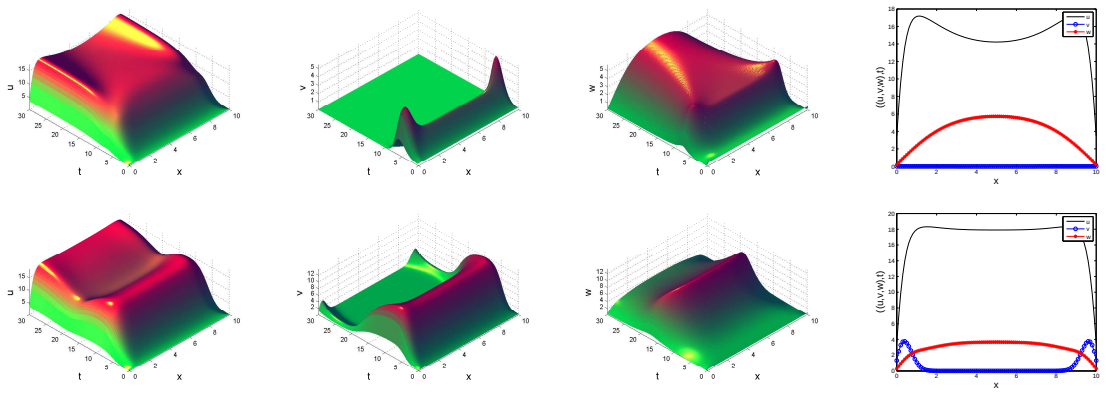


Figure 3: One dimensional evolution of species for the fractional reaction-diffusion system (1.1) at different instances of fractional index η. The upper and lower rows correspond to $\eta=1.25$ and $\eta=1.75$ respectively at $t=30$. The parameters are: $D_1=0.07$, $D_2=0.035$, $D_3=0.12$ and $\hat{w}=1/30$. Other parameter values as in (4.1) with initial conditions (4.2).

Table 1: Convergence of the ETD-ADAMS method for reaction-diffusion system (1.1) showing the effect of fractional derivative η.

Step size (Δx)	$Err(\Delta x,\Delta t=1/2048)$ at $\eta=1$	$Err(\Delta x,\Delta t=1/2048)$ at $\eta=1.5$
$\Delta x=1/2$	2.9698e-005	2.0021e-005
$\Delta x=1/4$	2.1925e-006	8.3166e-007
$\Delta x=1/8$	1.4894e-007	4.1151e-008
$\Delta x=1/16$	9.7055e-009	3.2240e-009
$\Delta x=1/32$	6.1969e-010	1.8337e-010

time step Δt at final time T and run some simulations with increasing number of the grid points. The l_∞ norm error is given by

$$Err(\Delta x,\Delta t)=||\bar{\omega}_c-\omega_c||_\infty$$

and reported for some values of Δx in Table 1. The parameters set as in (4.1) with $D_1=0.7$, $D_2=0.5$, $D_3=0.2$, $T=1$, and computed with initial data retained as in (4.2).

4.3 Two-dimensional example

In this section, we examine our numerical experiment in two dimensions by considering the fractional reaction-diffusion system (1.1). In the spirit of [44,45] in two dimensional space, subject to the clamped boundary conditions on $[0,L]\times[0,L]$, $L=200$, and the initial

https://doi.org/10.4208/aamm.OA-2016-0115 Published online by Cambridge University Press

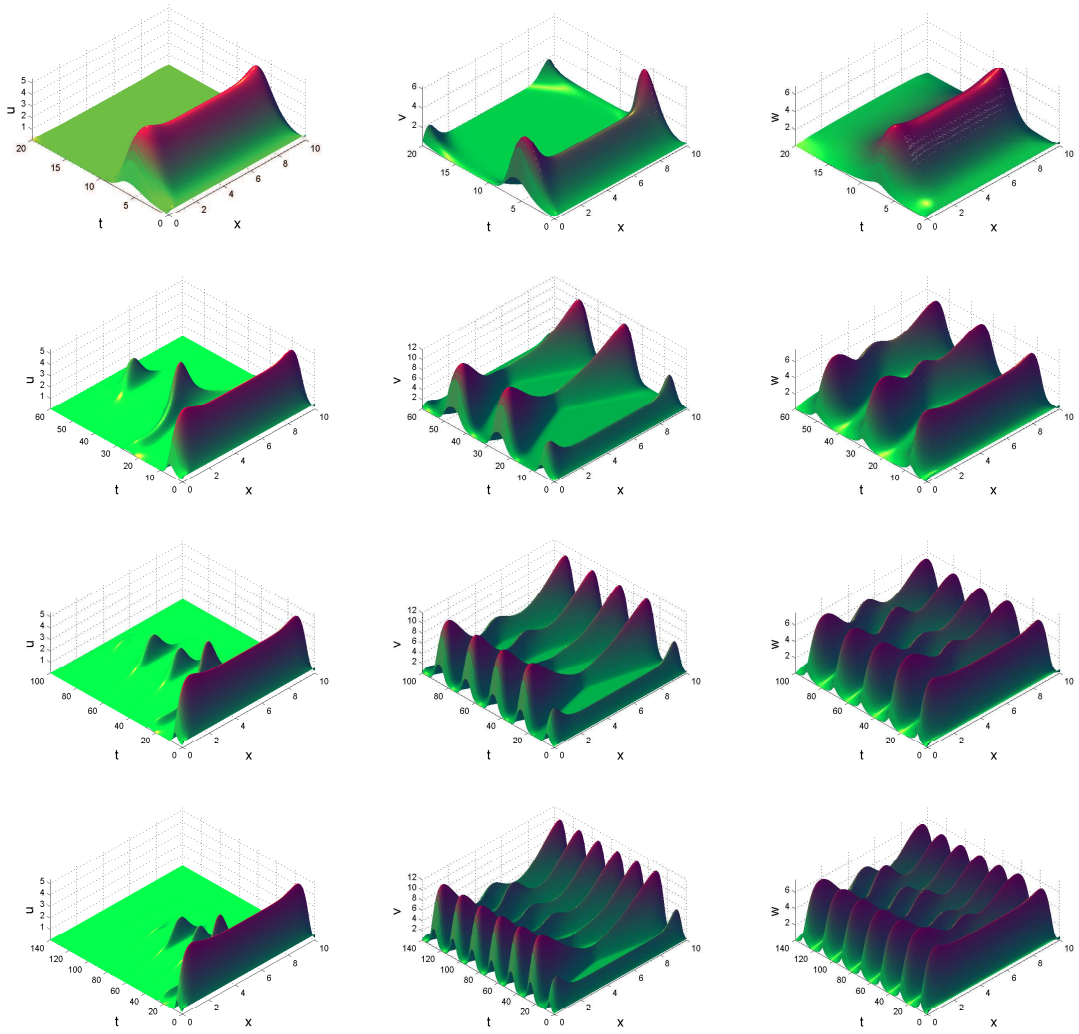


Figure 4: Different chaotic and complex spatiotemporal oscillations of the species evolving from the perturbation of the cropping rate α_i, $i=1,2$ with $\eta=1.50$ at some different instants of simulation time $t=20,60,100,140$. Other parameters and initial conditions are as given in Fig. 3 above.

conditions given as

$$u(x,y,0)=1-\frac{1}{30}\left[\sin\left(\frac{\pi x-\nu}{2\nu}\right)^{\omega}\times\sin\left(\frac{\pi y-\nu}{2\nu}\right)^{\omega}\right], \tag{4.3a}$$

$$v(x,y,0)=\frac{29}{360}\left[\sin\left(\frac{\pi x-\nu}{2\nu}\right)^{\omega}\times\sin\left(\frac{\pi y-\nu}{2\nu}\right)^{\omega}\right], \tag{4.3b}$$

$$u(x,y,0)=3-\frac{116}{245}\left[\sin\left(\frac{\pi x-\nu}{2\nu}\right)^{\omega}\times\sin\left(\frac{\pi y-\nu}{2\nu}\right)^{\omega}\right]. \tag{4.3c}$$

https://doi.org/10.4208/aamm.OA-2016-0115 Published online by Cambridge University Press

Ecological parameters used for the computations are give as

$$\begin{aligned}\{&\alpha_1=0.6,\ \alpha_2=0.8,\ \beta_1=1.5,\ \beta_2=2,\ \gamma_1=0.08,\ \gamma_2=0.05,\ \tau_1=0.9,\\ &\tau_2=1.2,\ \kappa_1=20,\ \kappa_2=15,\ \rho_1=0.35,\ \rho_2=0.45,\ \psi_1=0.15,\ \psi_2=0.25,\\ &\varphi_1=0.3,\ \varphi_2=0.7,\ \nu=0.5,\ \varpi=0.8,\ D_1=0.7,\ D_2=0.5,\ D_3=0.2,\ L=5\},\end{aligned}\tag{4.4}$$

In Fig. 5, the computer simulation of fractional reaction-diffusion systems (1.1) gives a strong evidence that pattern formation in the fractional reaction-diffusion case is almost the same as in classical reaction-diffusion equations, that is when $\eta=2$ [48]. The distributions of species in 2D here result to formation of spots which correspond to the one obtained by Murray [41]. In ecological sense, this result can be linked to the spot patterns on animals like Leopard and some birds. The results in the first, second and third rows correspond to the distributions of u, v and $w-$species at $\eta=1.25$, $\eta=1.55$ and $\eta=1.83$ respectively. It should be mentioned that formation of other Turing patterns such as stripes and pure spots are possible, depending on the choice of initial data and parameter values.

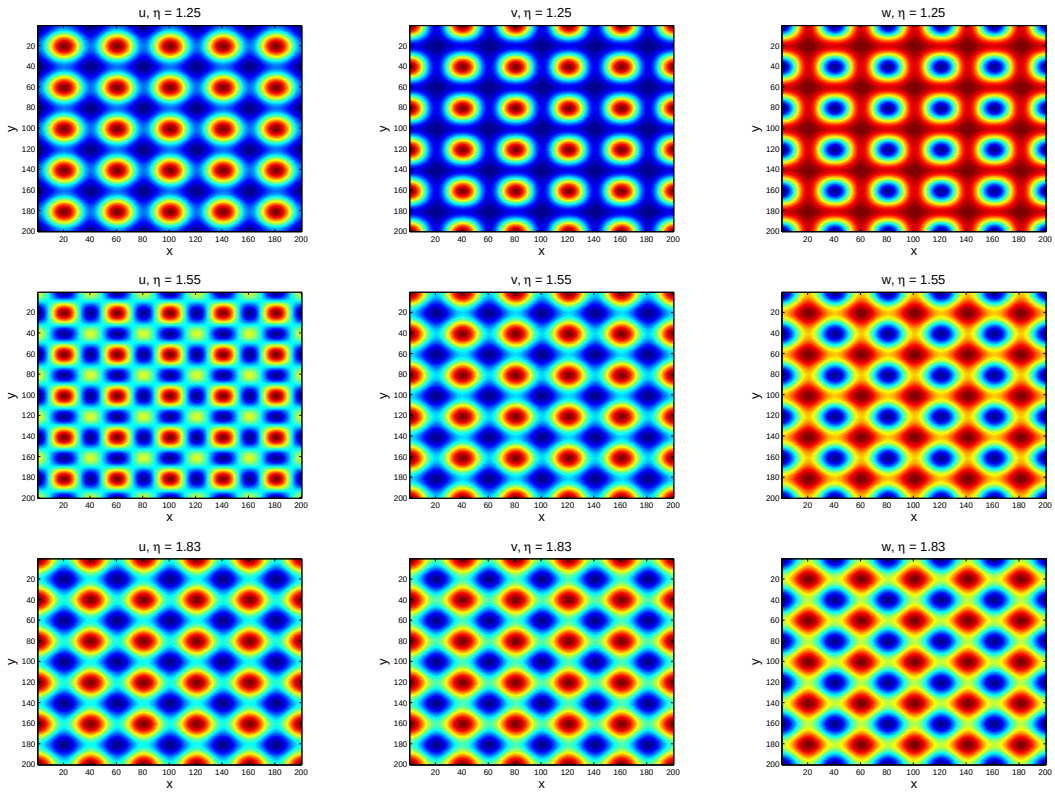


Figure 5: Two dimensional spots formation for fractional reaction-diffusion system (1.1) at different instants of $\eta=1.25,1.55,1.83$ which correspond to the upper-, middle- and lower-rows at $t=100$. Other parameters are as fixed in (4.4).

https://doi.org/10.4208/aamm.OA-2016-0115 Published online by Cambridge University Press

4.4 Three-dimensional example

Here, we explore the richness of different dynamics of the fractional predator-prey reaction-diffusion system (1.1) with kinetics (1.2), in three dimensions (3D). We let

$$\Delta^{\eta/2}=(\partial^{\eta/2}/\partial x^{\eta/2}+\partial^{\eta/2}/\partial y^{\eta/2}+\partial^{\eta/2}/\partial z^{\eta/2}),$$

for $u=(x,y,z,t)$, $v=(x,y,z,t)$ and $w=(x,y,z,t)$ subject to the initial functions

$$u(x,y,z,0)=1-\exp(-10((x-p/2)^2+(y-p/2)^2+(z-p/2)^2)), \tag{4.5a}$$

$$v(x,y,z,0)=\exp(-10((x-p/2)^2+2(y-p/2)^2+(z-p/2)^2)), \tag{4.5b}$$

$$w(x,y,z,0)=1.2-\exp(-10((x-p/2)^2+(y-p/2)^2+2.5(z-p/2)^2)). \tag{4.5c}$$

The nontrivial dynamics of the system was determined by the method of computer simulation showing the spatial evolution of the three species. The results of numerical simulation in 3D gives amazing scenarios for the distribution of different kinds of chaotic and spatiotemporal patterns in the parameter regime where pattern formation in the form of wavefront is partially driven by the fractional power index η. In the computational experiments, we use $128\times128\times128$ Fourier nodes on a $\pm L\times\pm L\times\pm L$ grid for $L=5$.

In Fig. 6, we noticed that the species distributions in 3D differ from one another, and as a result, we present our numerical analysis under the auspices of superdiffusive case at two instances of fractional power η and simulation time $t=10$. The upper-lower plots correspond to some chaotic and spatiotemporal patterns obtained for $\eta=1.25$ and $\eta=1.45$ respectively. A keen look reveals that the evolution of the species are not similar here,

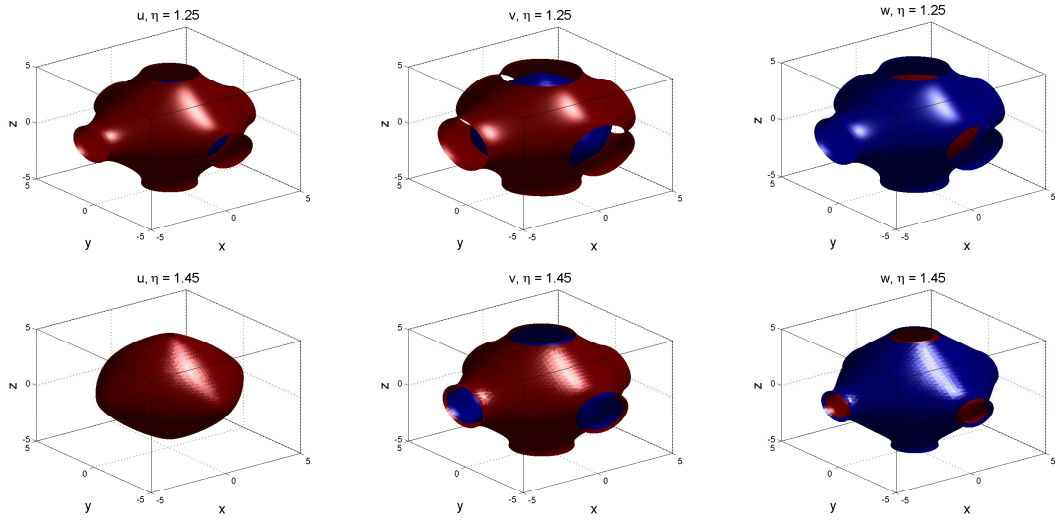


Figure 6: Three dimensional superdiffusive results of system (1.1) showing the spatial evolution of the species at two instances of fractional power η at $p=0.5$ and final time $t=10$. The upper-lower rows correspond to $\eta=1.25$ and $\eta=1.45$ respectively. Other parameters are given in (4.4) with initial conditions (4.5).

https://doi.org/10.4208/aamm.OA-2016-0115 Published online by Cambridge University Press

but it should be mentioned that other complex dynamical and more chaotic structures are obtainable by varying the initial and parameter data, as well as the fractional value η in the system.

5 Conclusions

In this paper, we have studied the dynamics of a reaction-diffusion system consisting of two preys and one predator spatial interactions. Mathematical analysis results have shown that the predator-prey system considered is locally asymptotically stable. We show that the mid-level predator and lowest-level prey washout periodic solution is globally asymptotically stable. It is of great interest that we have formulated a viable and efficient numerical schemes in both space and time, since the fractional reaction-diffusion equation can be split into diffusive stiff part and reaction moderately-stiff term. We formulate Fourier spectral method in space and integrate the resulting ODEs system in time with the exponential time differencing scheme whose formulation is based on the ADAMS-type method. Convergence result is displayed in Table 1. This research work has opened up some mathematical problems for other researchers to explore. At first, we suggest a theorem for system (1.1) to be globally asymptotically stable and permanent. Secondly, our methodology have also paved way to how such system of equations can be formulated in two and higher dimensions. Hence, we investigate the influences on the inherent spatiotemporal oscillation caused as a result of impulsive perturbation. Computer simulation experiment of the fractional-in-space reaction-diffusion systems in one, two and three dimensions has given enough and provide a good evidence that pattern formation in the fractional regime $(1 < \eta \leq 2)$ is almost the same as in the case of classical reaction-diffusion system when $(\eta = 2)$. To keep the study open for researchers to explore, we present via theorems the conditions for system (1.1) to be globally asymptotically stable and permanent. For future research, the methodology presented in this paper can serve as a good working template to solve any fractional reaction-diffusions problems in higher dimensions.

Acknowledgments

The authors would like to thank the referees for their helpful suggestions.

References

[1] A. ATANGANA, *On the stability and convergence of the time-fractional variable order telegraph equation*, J. Comput. Phys., 293 (2015), pp. 104–114.
[2] A. ATANGANA, *On the new fractional derivative and application to Fisher's reaction-diffusion*, Appl. Math. Comput., 273 (2016) 948-956.

https://doi.org/10.4208/aamm.OA-2016-0115 Published online by Cambridge University Press

[3] A. ATANGANA AND D. BALEANU, *New fractional derivatives with nonlocal and non-singular kernel: Theory and application to heat transfer model,* Thermal Science, 20 (2016), pp. 763–769.
[4] A. ATANGANA AND I. KOCA, *Chaos in a simple nonlinear system with Atangana-Baleanu derivatives with fractional order,* Chaos, Solitons & Fractals, 89 (2016), pp. 447–454.
[5] W. ARNOLDI, *The principle of minimized iteration in the solution of the matrix eigenvalue problem,* Quarterly Appl. Math., 9 (1951), pp. 17–29.
[6] D. D. BAINOV AND P. C. SIMEONOV, Impulsive Differential Equations: Asymptotic Properties of the Solutions, World Scientific, Singapore, 1993.
[7] D. BALEANU, A. GOLMANKHANEH, R. NIGMATULLIN AND A. GOLMANKHANEH, *Fractional newtonian mechanics,* Open Phys., 8 (2010), pp. 120–125.
[8] A. H. BHRAWY, M. A. ZAKY, D. BALEANU AND M. A. ABDELKAWY, *A novel spectral approximation for the two-dimensional fractional sub-diffusion problems,* Rom. J. Phys., 60 (2015), pp. 344–359.
[9] A. H. BHRAWY, *An efficient Jacobi pseudospectral approximation for nonlinear complex generalized Zakharov system,* Appl. Math. Comput., 247 (2014), pp. 30–46.
[10] A. H. BHRAWY, E. H. DOHA, D. BALEANU AND S. S. EZZ-ELDEIN, *A spectral tau algorithm based on Jacobi operational matrix for numerical solution of time fractional diffusion-wave equations,* J. Comput. Phys., 293 (2015), pp. 142–156.
[11] A. H. BHRAWY, *A Jacobi spectral collocation method for solving multi-dimensional nonlinear fractional sub-diffusion equations,* Numer. Algorithms, 17 (2016), pp. 91–113. DOI: 10.1007/s11075-015-0087-2
[12] A. H. BHRAWY, *A new spectral algorithm for a time-space fractional partial differential equations with subdiffusion and superdiffusion,* Proceedings of the Romanian Academy A, 17 (2016), pp. 39–46.
[13] J. P. BOYD, Chebyshev and Fourier Spectral Methods, Dover, Mineola, New York, 2001.
[14] A. BUENO-OROVIO, D. KAY AND K. BURRAGE, *Fourier spectral methods for fractional-in-space reaction-diffusion equations,* BIT Numer. Math., 54 (2014), pp. 937–954.
[15] R. S. CANTRELL AND C. COSNER, *Permanence in ecological systems with spatial heterogeneity,* Proc. Roy. Soc. Edinburgh, 123A (1993), pp. 533–559.
[16] Y. Chang, W. Feng, M. Freeze and X. Lu, Permanence and coexistence in a diffusive complex ratio-dependent food chain, Int. J. Dyn. Control Systems, DOI:10.1007/s40435-014-0131-4 (2014).
[17] S. M. COX AND P. C. MATTHEWS, *Exponential time differencing for stiff systems,* J. Comput. Phys., 176 (2002), pp. 430–455.
[18] E. N. DANCER, *The existence and Uniqueness of positive solutions of competing species equations with diffusion,* Trans. Amer. Math. Soc., 326 (1991), pp. 829–859.
[19] E. H. DOHA, A. H. BHRAWY, D. BALEANU AND R. M. HAFEZ, *A new Jacobi rational-Gauss collocation method for numerical solution of generalized pantograph equations,* Appl. Numer. Math., 77 (2014), pp. 43–54.
[20] Q. DU AND W. ZHU, *Analysis and applications of the exponential time differencing schemes and their contour integration modifications,* BIT Numer. Math., 45 (2005), pp. 307–328.
[21] W. FENG, *Permanence effect in a three-species food chain model,* Appl. Anal., 54 (1994), pp. 195–209.
[22] W. FENG, C. V. PAO AND X. LU, *Global attractors of reaction-diffusion system modeling food chain populations with delays,* Commun. Pure Appl. Anal., 10, pp. 1463–1478.
[23] W. FENG, M. T. COWEN AND X. LU, *Coexistence and asymptotic stability in age-structured predator-prey models,* Math. Biosci. Eng., 11 (2014), pp. 823–839.

https://doi.org/10.4208/aamm.OA-2016-0115 Published online by Cambridge University Press

[24] B. FORNBERG, A practical Guide to Pseudospectral Methods, Cambridge University Press, Cambridge, 1998.
[25] M. GARVIE, *Finite-difference schemes for reaction-diffusion equations modeling predator-pray interactions in MATLAB,* Bull. Math. Bio., 69 (2007), pp. 931–956.
[26] J. F. GÓMEZ-AGUILAR, M. G. LÓPEZ-LÓPEZ, V. M. ALVARADO-MARTÍNEZ, J. REYES-REYES AND M. ADAM-MEDINA, *Modeling diffusive transport with a fractional derivative without singular kernel,* Phys. A Stat. Mech. Appl., 447 (2016), pp. 467–481.
[27] J. F. GÓMEZ-AGUILAR, L. TORRES, H. YÉPEZ-MARTÍNEZ, D. BALEANU, J. M. REYES AND I. O. SOSA, *Fractional Linard type model of a pipeline within the fractional derivative without singular kernel,* Adv. Difference Equations, 2016(1) (2016), pp. 1–13.
[28] M. HAQUE, *Ratio-dependent predator-prey models of interacting populations,* Bull. Math. Bio., 71 (2009), pp. 430–452.
[29] B. I. HENRY AND S. L. WEARNE, *Fractional reaction-diffusion,* Phys. A Stat. Mech. Appl., 276 (2000), pp. 448–455.
[30] M. HOCHBRUCK AND A. OSTERMANN, *Exponential integrators,* Acta Numer., 19 (2010), pp. 209–286.
[31] M. HOCHBRUCK AND A. OSTERMANN, *Exponential multistep methods of Adams-type,* BIT Numer. Math., 51 (2011), pp. 889–908.
[32] W. R. HOLMES, *An efficient, nonlinear stability analysis for detecting pattern formation in reaction diffusion systems,* Bull. Math. Bio., 76 (2014), pp. 157–183.
[33] R. D. HOLT, *Predation, apparent competition, and the structure of prey communities,* Theoretical Population Biology, 12 (1997), pp. 197–229.
[34] J. JIAO, L. CHEN AND L. LI, *Asymptotic behavior of solutions of second-order nonlinear impulsive differential equations,* J. Math. Anal. Appl., 331 (2008), pp. 458–463.
[35] A. KASSAM AND L. N. TREFETHEN, *Fourth-order time-stepping for stiff PDEs,* SIAM J. Sci. Comput., 26 (2005), pp. 1214–1233.
[36] V. LAKSHMIKANTHAM, D. D. BAINOV AND P. C. SIMEONOV, Theory of Impulsive Differential Equations, World Scientific, Singapore, 1989.
[37] A. LEUNG, *Limiting behaviour for a prey-predator model with diffusion and crowding effects,* J. Math. Bio., 6 (1978), pp. 87–93.
[38] A. LEUNG, Systems of Nonlinear Partial Differential Equations, Kluwer Publisher, Boston, 1989.
[39] V. F. MORALES-DELGADO, J. F. GÓMEZ-AGUILAR, H. YÉPEZ-MARTÍNEZ, D. BALEANU, R. F. ESCOBAR-JIMENEZ AND V. H. OLIVARES-PEREGRINO, *Laplace homotopy analysis method for solving linear partial differential equations using a fractional derivative with and without kernel singular,* Adv. Difference Equations, 2016 (1), (2016).
[40] M. L. MORGADO AND M. REBELO, *Numerical approximation of distributed order reaction-diffusion equations,* J. Comput. Appl. Math., 275 (2015), pp. 216–227.
[41] J. D. MURRAY, Mathematical Biology II: Spatial Models and Biomedical Applications, Springer-Verlag, Berlin, 2003.
[42] K. M. OWOLABI AND K. C. PATIDAR, *Higher-order time-stepping methods for time-dependent reaction-diffusion equations arising in biology,* Appl. Math. Comput., 240 (2014), pp. 30–50.
[43] K. M. OWOLABI, *Robust IMEX schemes for solving two-dimensional reaction-diffusion models,* Int. J. Nonlinear Sci. Numer. Simulations, 16 (2015), pp. 271–284.
[44] K. M. OWOLABI AND K. C. PATIDAR, *Existence and permanence in a diffusive KiSS modelwith robust numerical simulations,* Int. J. Differential Equations, (2015), 485860, doi:10.1155/2015/485860.

https://doi.org/10.4208/aamm.OA-2016-0115 Published online by Cambridge University Press

[45] K. M. Owolabi and K. C. Patidar, *Numerical simulations of multicomponent ecological models with adaptive methods,* Theoret. Bio. Medical Model., 13 (2016), 1. DOI 10.1186/s12976-016-0027-4.
[46] K. M. Owolabi and A. Atangana, *Numerical solution of fractional-in-space nonlinear Schrodinger equation with the Riesz fractional derivative,* The Euro. Phys. J. Plus, 131 (2016), 335. Doi:10.1140/epjp/i2016-16335-8.
[47] K. M. Owolabi, *Mathematical analysis and numerical simulation of patterns in fractional and classical reaction-diffusion systems,* Chaos, Solitons and Fractals, 93 (2016), pp. 89–98.
[48] K. M. Owolabi, *Robust and adaptive techniques for numerical simulation of nonlinear partial differential equations of fractional order,* Commun. Nonlinear Sci. Numer. Simulations, 44 (2017), pp. 304–317.
[49] E. Pindza, K. M. Owolabi, *Fourier spectral method for higher order space fractional reaction-diffusion equations,* Commun. Nonlinear Sci. Numer. Simulation, 40 (2016), pp. 112–128.
[50] Y. Saad, *Analysis of some Krylov susbspace approximations to the matrix exponential operator,* SIAM J. Numer. Anal., 131 (1992), pp. 209–228.
[51] R. A. Satnoianu, M. Menzinger and P. K. Maini, *Turing istabilities in general systems,* J. Math. Bio., 41 (2000), pp. 493–512.
[52] G. Sun, G. Zhang, Z. Jin and L. Li, *Predator cannibalisms can give rise to regular spatial patterns in a predator-prey system,* Nonlinear Dyn., 58 (2009), pp. 75–84.
[53] S. Sun and L. Chen, *Permanence and complexity of the Eco-Epidemiological model with impulsive perturbation,* Int. J. Biomath., 1 (2008), pp. 121–132.
[54] L. N. Trefethen, Spectral Methods in MATLAB, SIAM, Philadelphia, 2000.
[55] V. V. Uchaikin, Fractional Derivatives for Physicists and Engineers, Springer, Berlin, 2013.
[56] V. Volpert and S. Petrovskii, *Reaction-diffusion waves in biology,* Phys. Life Reviews, 6 (2009), pp. 267–310.
[57] H. Wang and W. Wang, *The dynamical complexity of a Ivler-type prey-predator system with impulsive effect,* Chaos Solitons & Fractals 38 (2008), pp. 1168–1176.
[58] L. Wang, L. Chen and J. J. Nieto, *The dynamics of an epidemic model for pest control with impulsive effect,* Nonlinear Analysis: Real World Applications, (2010), pp. 1374–1386.
[59] J. A. C. Weideman and S. C. Reddy, *A MATLAB differentiation matrix suite,* ACM Trans. Math. Software, 26 (2001), pp. 465–519.
[60] G. C. Wu, D. Baleanu, S. D. Zeng and Z. G. Deng, *Discrete fractional diffusion equation,* Nonlinear Dyn., 80 (2015), pp. 281–286.
[61] H. Yu, S. Zhong and M. Ye, *Dynamic analysis of an ecological model with impulsive control strategy and distributed time delay,* Math. Comput. Simulation, 80 (2009), pp. 619–632.
[62] H. Yu, S. Zhong, M. Ye and W. Chen, *Mathematical and dynamic analysis of an ecological model with an impulsive control strategy and distributed time delay,* Math. Comput. Model., 50 (2009), pp. 1621–1635.
[63] H. Yu, S. Zhong and R. P. Agarwal, *Mathematical Analysis of an apparent competition community model with impulsive effect,* Math. Comput. Model., 52 (2010), pp. 25–36.
[64] H. Yu, S. Zhong, R. P. Agarwal and L. Xiong, *Species permanence and dynamical behavior analysis of an impulsively controlled ecological system with distributed time delay,* Comput. Math. Appl., 59 (2010), pp. 3824–3835.

https://doi.org/10.4208/aamm.OA-2016-0115 Published online by Cambridge University Press